

# Self-motile colloidal particles: from directed propulsion to random walk

Jonathan R. Howse,<sup>1</sup> Richard A.L. Jones,<sup>1,\*</sup> Anthony J. Ryan,<sup>2</sup>  
Tim Gough,<sup>3</sup> Reza Vafabakhsh,<sup>4</sup> and Ramin Golestanian<sup>1,†</sup>

<sup>1</sup>*Department of Physics and Astronomy, University of Sheffield, Sheffield S3 7RH, UK*

<sup>2</sup>*Department of Chemistry, University of Sheffield, Sheffield S3 7HF, UK*

<sup>3</sup>*IRC in Polymer Engineering, University of Bradford, BD7 1DP, UK*

<sup>4</sup>*Institute for Advanced Studies in Basic Sciences, Zanjan 45195-1159, Iran*

(Dated: February 1, 2008)

The motion of an artificial micro-scale swimmer that uses a chemical reaction catalyzed on its own surface to achieve autonomous propulsion is fully characterized experimentally. It is shown that at short times, it has a substantial component of directed motion, with a velocity that depends on the concentration of fuel molecules. At longer times, the motion reverts to a random walk with a substantially enhanced diffusion coefficient. Our results suggest strategies for designing artificial chemotactic systems.

PACS numbers: 07.10.Cm, 87.19.St, 82.39.-k, 87.17.Jj

The directed propulsion of small scale objects in water is problematic because of the combination of low Reynolds number and Brownian motion on these length scales [1]. In order to achieve an artificial micro- or nano-scale swimmer that is able to propel itself in a purposeful way, one needs both a swimming strategy that works in the environment of low Reynolds number [2], and a strategy for steering and directing the motion that can overcome the ubiquity of Brownian motion. Common bacteria, such as *E. Coli*, achieve propulsion by non-time-reversible motion of long flagella, and employ a “run and tumble” strategy to be able to swim towards or away from environmental stimuli [3].

One possibility for designing propulsion is to devise non-reciprocal deformation strategies that are simple enough to be realizable [4]. Recently, an interesting example of such robotic micro-swimmers has been made using magnetic colloids attached by DNA-linkers, and controlled by an external oscillatory magnetic field [5]. Another possibility is to take advantage of *phoretic* effects, where gradients of fields such as concentration, temperature, electric field, etc, couple to the surface properties of particles to create slip velocity patterns that could lead to net propulsion [6].

A particularly appealing strategy for propelling small devices is to take advantage of chemical reactions [7]. In a pioneering experiment, Paxton *et al.* observed autonomous motion of platinum/gold nanorods [8], and similar experiments have been performed by Fourneir-Bodoz *et al* who used gold/nickel nanorods [9] and Mano and Heller who used enzymes [10]. One simple strategy for converting chemical energy to mechanical work in such devices has been proposed by one of us and collaborators [11, 12]. In this scheme, a spherical particle is considered with an asymmetric distribution of catalyst on its surface. If the chemical reaction so catalyzed produces more products than it has reactants, then the asymmetric distribution of reaction products propels the particle by a

process of *self-diffusiophoresis*. The experimentally realized swimmers mentioned above are very similar in setup to the one proposed in Ref. [11]. However, it seems that the driving mechanism for the propulsion in these experiment is different as it depends strongly on the presence of a (bi-metal or bio-) electro-catalytic structure [13]. It is suggested that the pair of electrochemical reactions at the two poles create a lateral electric field near the particle surface (due to electron transfer) that could move the solvent via electro-osmosis [13].

Here we have realized the scheme proposed in Ref. [11] experimentally by taking polystyrene spheres with narrow size distributions with a diameter of  $1.62\mu\text{m}$ , and coating one side of the spheres with platinum keeping the second half as the non-conducting polystyrene. The platinum catalyzes the reduction of a “fuel” of hydrogen peroxide to oxygen and water, which produces more molecules of reaction product than consumed fuel. We fully characterize the motion of the artificial micro-scale swimmer using particle tracking, and probe the properties of the motion as a function of hydrogen peroxide concentration. We show that at short times, the particles move predominantly in a directed way, with a velocity that depends on the concentration of the fuel molecules

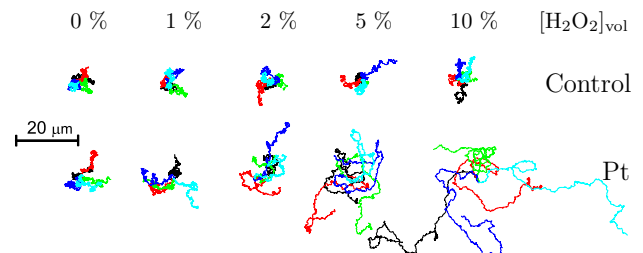


FIG. 1: (color online). Trajectories over 25 sec for  $\times 5$  particles of the control (blank) and Platinum-coated particles in water, and varying solutions of hydrogen peroxide.

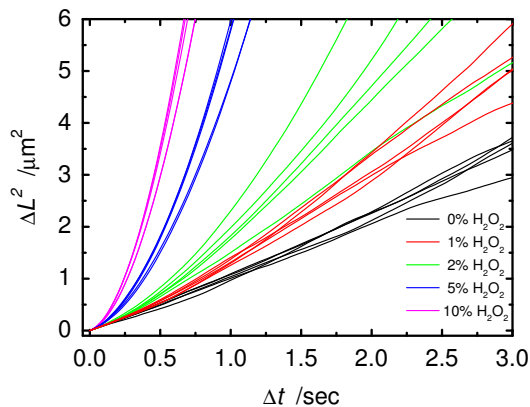


FIG. 2: (color). Mean squared displacement as a function of time interval for the Pt-coated sphere trajectories shown in Fig. 1, corresponding to different hydrogen peroxide concentrations.

with a Michaelis-Menten behavior. At longer times, the motion reverts to a random walk, in which runs of directed motion are interrupted by random changes of direction. We also extract the positional and the rotational diffusion coefficients and show that they are consistent with theoretical predictions, with the rotational diffusion featuring a moderate concentration dependence that could be attributed to directed rotational components in the motion.

Polystyrene microspheres were produced as described by Fujii et al [14]. The weight-average diameter of the microspheres was determined by dynamic light scattering to be  $1.62 \pm 0.13 \mu\text{m}$ , with a polydispersity index of 1.008. To half-coat the spheres [15] in platinum, a dilute suspension (0.05 wt%) of the spheres in isopropanol (HPLC grade: Fischer) was drawn over cleaned glass microscope slides to produce a dilute monolayer of the spheres ( $\sim 10^5$  spheres $\cdot\text{cm}^{-2}$ ). A thin layer of Platinum (99.99% Agar Scientific) was evaporated onto the microsphere coated slides resulting in a layer of Platinum 5.5 nm thick on one side of the spheres. The half-platinum coated spheres were detached from the glass slide using a sheet of PTFE (200  $\mu\text{m}$  thick - Goodfellows) acting as a blade and the detached spheres resuspended in 2 ml of distilled water (18.2  $\text{M}\Omega \text{cm}^{-1}$  - Purite). Hydrogen peroxide solutions were prepared by subsequent dilutions of 30 % Hydrogen Peroxide solution (Perdrogen - Riedel-de Haën). For a given solution of hydrogen peroxide, 100  $\mu\text{l}$  of the microsphere containing stock solution was mixed with 2 ml of the appropriate solution. A cuvette (1 mm optical path length - Hellma, cleaned with Piranha Etch) was rinsed three times with the solution before filling again and sealed using a PTFE stopper. Particle tracking was achieved using a Nikon ME600 optical microscope mounted on an isolation table and fitted with a Pixelink PL-A742 machine vision camera, a  $\times 20$  objective (Nikon), and inverted illumination. A movie

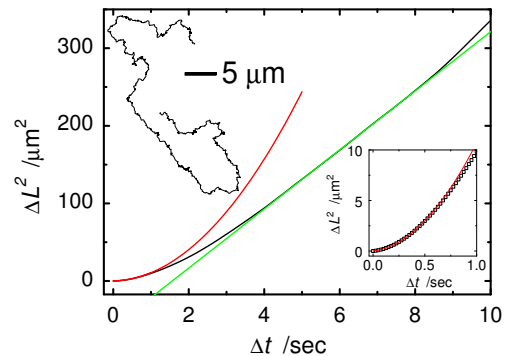


FIG. 3: (color online). Mean squared displacement as a function of time for the inset trajectory (Pt-coated sphere in 10%  $\text{H}_2\text{O}_2$ ) fitted to Eq. (1), which resembles a parabola (red line) at  $\Delta t \ll \tau_R$  and a straight line (green line) at  $\Delta t \gg \tau_R$ . The fits yield  $v = 3.1 \mu\text{m s}^{-1}$ ,  $D = 0.31 \mu\text{m}^2\text{s}^{-1}$ , and  $\tau_R = 3.9 \text{ s}$  for this particular trajectory.

with a field of view of approximately  $120 \mu\text{m} \times 120 \mu\text{m}$  of 3000 frames at a rate of 38 frames per second was recorded for each particle. For each concentration of hydrogen peroxide approximately 20 separate particles were tracked and analyzed using a Labview (National Instruments) script providing particle trajectory and timing (time,  $x/\mu\text{m}$ , and  $y/\mu\text{m}$ ).

Figure 1 shows particle traces for a Pt-coated bead as well as a control polystyrene bead. While the control particle undergoes a characteristic Brownian motion, the Pt-coated particle shows a systematic enhancement of a directional component in its motion, as the concentration of hydrogen peroxide increases [16]. The motion can be analyzed more quantitatively using particle tracking. From the records of the particle trajectory, we calculate the average value of the squared displacement as a function of time. For a purely Brownian particle of radius  $R$ , the squared displacement is linear in time with the slope controlled by the particle diffusion coefficient  $D = k_B T / (6\pi\eta R)$ , where  $k_B T$  is the thermal energy,  $\eta$  is the viscosity of water. The particle will also undergo rotational diffusion with a characteristic (inverse) time scale  $\tau_R^{-1} = k_B T / (8\pi\eta R^3)$  (also called the rotational diffusion coefficient), with the two stochastic modes decoupled from each other. For a particle propelled with velocity  $V$ , the direction of motion is itself subject to rotational diffusion that leads to a coupling between rotation and translation. In this case, one can show that the (2D projection) mean squared displacement is given as:

$$\Delta L^2 = 4D\Delta t + \frac{V^2\tau_R^2}{2} \left[ \frac{2\Delta t}{\tau_R} + e^{-2\Delta t/\tau_R} - 1 \right]. \quad (1)$$

This expression has limiting forms of  $\Delta L^2 = 4D\Delta t + V^2\Delta t^2$  for  $\Delta t \ll \tau_R$  and  $\Delta L^2 = (4D + V^2\tau_R)\Delta t$  for  $\Delta t \gg \tau_R$ . At short times, the contribution to the displacement due to the propulsion is linear in time, while

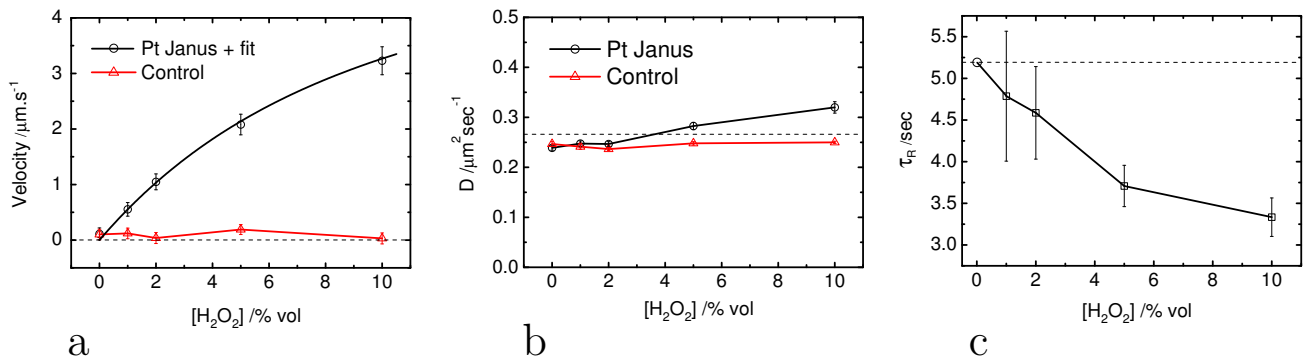


FIG. 4: (color online). (a) Velocity determined from the  $\Delta t \ll \tau_R$  behavior for the control ( $\Delta$ ) and Pt-coated particles ( $\circ$ ). The solid line is the line of best fit using Eqs. (2) and (3), with  $a = 1.2\text{\AA}$ ,  $\lambda = 5\text{\AA}$ ,  $k_1 = 4.4 \times 10^{11} \mu\text{m}^{-2}\text{s}^{-1}$ , and  $k_2 = 4.8 \times 10^{10} \mu\text{m}^{-2}\text{s}^{-1}$ . (b) Diffusion coefficient determined from the  $\Delta t \ll \tau_R$  behavior for the control and Pt-coated particles with the theoretical value (—) indicated. (c) Rotational diffusion time determined at  $\Delta t \gg \tau_R$  (from the gradient). Value at  $[\text{H}_2\text{O}_2]=0$  is the theoretical value.

the Brownian displacement is proportional to the square root of time, with these two contributions adding in quadrature. At times long compared to the rotational diffusion time, rotational diffusion leads to a randomization of the direction of propulsion, and the particle undergoes a random walk whose step length is the product of the propelled velocity  $V$  and the rotational diffusion time, leading to a substantial enhancement of the effective diffusion coefficient over the classical value, namely  $D_{\text{eff}} = D + \frac{1}{4}V^2\tau_R$ . A similar crossover behavior has been observed in the motion of tracer beads in the flow caused near surfaces covered by bacterial carpets, as well as beads propelled by adsorbed bacteria [17].

Figure 2 shows the average mean squared displacement as a function of elapsed time for half-coated particles immersed in hydrogen peroxide at various concentrations. Each curve in Fig. 2 is produced by averaging over 3000 frames. In the absence of hydrogen peroxide, the curves are linear, indicating the simple diffusive behavior expected of a particle undergoing Brownian motion. With the addition of hydrogen peroxide they show an increasingly important parabolic component; the particles are being propelled by the local osmotic pressure gradient created by the asymmetric chemical reaction. Fitting these plots to the limiting forms of the interpolation formula of Eq. (1) yields values for the parameters ( $V$ ,  $D$ , and  $\tau_R$ ) as functions of  $\text{H}_2\text{O}_2$  concentration (see Fig. 3). For each concentration, we perform averaging over 20 independent movies for the values of the fitting parameters.

Figure 4a shows the propulsion velocity as a function of the hydrogen peroxide concentration. As we expect, as the concentration of “fuel” rises the velocity with which the Pt half-coated particles are propelled rises from the value of zero observed in the absence of fuel; for the control particles, without catalyst, no propulsion is observed. The propulsion velocity can be calculated using the lateral gradient of the excess solute concentration  $C$  in the

vicinity of the particle surface. This gradient creates a slip velocity  $V_s = \mu\partial_{\parallel}C$  with the diffusio-phoretic mobility given as  $\mu = k_B T \lambda^2 / \eta$  where  $\lambda$  represents the range of the interaction zone between the solute and the particle [18]. One can then solve the Stokes hydrodynamics around the sphere subject to this local slip velocity pattern on its surface, and find the propulsion velocity. For a particle which is half-coated with a material that can produce excess particles with diffusion coefficient  $D_o$  at a rate per unit area  $k$ , the propulsion velocity is [12]:

$$V = \frac{\mu k}{4D_o} = \frac{3\pi}{2} k a \lambda^2, \quad (2)$$

where the hydrodynamic radius of the solute  $a$  is introduced by way of the Stokes-Einstein relation.

Since the velocity is directly proportional to the effective surface reaction-rate  $k$  [Eq. (2)], the linear initial increase and the subsequent tendency towards saturation observed in Fig. 4a suggests that the Pt-catalyzed breakdown of  $\text{H}_2\text{O}_2$  probably occurs in two stages of formation of a  $\text{Pt}(\text{H}_2\text{O}_2)$  complex at a rate per unit area  $k_1[\text{H}_2\text{O}_2]_{\text{vol}}$ , in which  $[\text{H}_2\text{O}_2]_{\text{vol}}$  has the units of volume percentage, followed by a decomposition into water and oxygen at a rate per unit area  $k_2$ . This leads to a Michaelis-Menten behavior similar to enzymes [19], as opposed to the kinetics of decomposition in homogenous solution, which is second order and would produce an upward curvature in Fig. 4a. Solving the diffusion-reaction equations with the proposed reaction kinetics, we find

$$k = k_2 \frac{[\text{H}_2\text{O}_2]_{\text{vol}}}{[\text{H}_2\text{O}_2]_{\text{vol}} + k_2/k_1}. \quad (3)$$

The solid line in Fig. 4a is obtained from equations (2) and (3), with  $a = 1.2\text{\AA}$ ,  $\lambda = 5\text{\AA}$ ,  $k_1 = 4.4 \times 10^{11} \mu\text{m}^{-2}\text{s}^{-1}$ , and  $k_2 = 4.8 \times 10^{10} \mu\text{m}^{-2}\text{s}^{-1}$ , which are reasonable numbers. In contrast to the strong dependence of the propulsion velocity on hydrogen peroxide,

the fitted particle (bare) diffusion coefficient  $D$  shown in Fig. 4b has little dependence on the presence or absence of catalyst and the concentration of hydrogen peroxide, and is close to the predicted value from Einstein-Stokes relation (a slight residual dependence on hydrogen peroxide concentration may be a result of a coupling between these two fitting parameters in the analysis of the displacement curves). Figure 4c shows fitted rotational diffusion time. As mentioned above, the long time effective diffusion is substantially enhanced due to the propulsion. For the largest hydrogen peroxide concentration, we find a value of  $D_{\text{eff}} = 9.0 \mu\text{m}^2\text{s}^{-1}$ , which is an enhancement over the purely Brownian value  $D$  by a factor of nearly 30.

The rotational diffusion time shows a systematic decrease as a function of hydrogen peroxide concentration for the coated particles, with no dependence for the controls. This could be due to the surface reaction imparting a small net angular velocity  $\omega$ , and we surmise that it might be caused by inadvertent asymmetric Pt coverage during the fabrication. Similar to the translational diffusion coefficient, we would expect a combination  $\tau_{\text{R}}^{-1} + \omega^2\tau_{\text{R}}$  to serve as the renormalized rotational diffusion coefficient. This hypothesis is strengthened by the observation of cycloid trajectories for some samples at high  $\text{H}_2\text{O}_2$  concentrations. At first sight this would seem an unwelcome side effect—an increase in rotational velocity has the effect of decreasing the renormalized diffusion coefficient for the long-time behavior of the propelled particles. But it also raises the intriguing possibility of designing a system in which the linear propulsive and rotational behavior are independently controlled; this would constitute a system in which the step size of a random walk could be controlled by an external parameter, opening up the possibility of designing a system capable of chemotaxis, in a way analogous to the bacteria *E. Coli* [3].

By contrast to the existing experimental examples of autonomous swimmers [8, 9, 10, 13], the propulsion mechanism for our platinum/polystyrene particles does not involve electrochemical reactions, and thus they realize a new class of micro- and nano-scale chemical locomotion. We note that for this class of (self-diffusiophoretic) swimmers, spherical geometry is better than a rod geometry, because the velocity for rods is reduced by a factor of the aspect ratio [12]. Moreover, their true directional motion is easier to resolve experimentally as the lower friction coefficient of the rods along their length causes them to spend more time going along their own direction, which in short time probing might be mistaken with directional locomotion.

In conclusion, we show that spatially asymmetric catalysis at the surface of synthetic micron-scale particles can lead to effective autonomous propulsion of spherical colloids. At short times, we observe directed propulsion of the particles with velocities in the  $\mu\text{m}/\text{s}$  range; at longer

times the direction of motion of the particles is randomized, and the motion of the particles becomes diffusive in character with an effective diffusion coefficient which is substantially enhanced over the Brownian value. We hope that our quantitative characterization of the motion of the swimmer sheds some light on the fundamental issues involved in designing chemical locomotive systems, and could inspire new directions for their implementation.

R.G. acknowledges V. Sanei and M.T. Sarbolouki for their help during the early stages of the experiment. This work was supported by the EPSRC.

---

\* Electronic address: r.a.l.jones@sheffield.ac.uk

† Electronic address: r.golestanian@sheffield.ac.uk

- [1] E.M. Purcell, American Journal of Physics **45**, 3-11 (1977).
- [2] G.I. Taylor, Proc. Roy. Soc. London **A 209**, 447-461 (1951).
- [3] H.C. Berg, *Random Walks in Biology* (Princeton University Press, Princeton, NJ, 1983).
- [4] For a simple example, among others, see: A. Najafi and R. Golestanian, Phys. Rev. E **69**, 062901 (2004).
- [5] R. Dreyfus, J. Baudry, M.L. Roper, M. Fermigier, H.A. Stone, J. Bibette, Nature **437**, 862 (2005).
- [6] J.L. Anderson, Ann. Rev. Fluid Mech. **21**, 61 (1989).
- [7] W.F. Paxton *et al.*, Angew. Chem. Int. Ed. **45**, 5420 (2006), and references therein.
- [8] W.F. Paxton, *et al.* J. Am. Chem. Soc. **126**, 13424 (2004).
- [9] S. Fournier-Bidoz, A.C. Arsenault, I. Manners, and G.A. Ozin, Chem. Comm., 441-443 (2005).
- [10] N. Mano and A. Heller, J. Am. Chem. Soc. **127**, 11574 (2005).
- [11] R. Golestanian, T.B. Liverpool, and A. Ajdari, Phys. Rev. Lett. **94**, 220801 (2005).
- [12] R. Golestanian, T.B. Liverpool, and A. Ajdari, New J. Phys. **9**, 126 (2007).
- [13] W.F. Paxton, A. Sen, T.E. Mallouk, Chemistry - a European Journal **11**, 6462 (2005).
- [14] S. Fujii, P.D. Iddon, A.J. Ryan, and S.P. Armes, Langmuir **22**, 7512 (2006).
- [15] A. Perro *et al.*, Journal of Materials Chemistry **15**, 3745 (2005).
- [16] See EPAPS Document No. [xxxxxxx] for supplementary Video, which can be reached via a direct link in the online article's HTML reference section or via the EPAPS homepage (<http://www.aip.org/pubservs/epaps.html>). It shows particle motion for both control (upper row) and platinum-coated (lower row) spheres in water (left column) and 10%  $\text{H}_2\text{O}_2$  (right column). x-axis=y-axis=127  $\mu\text{m}$ , speed of movie running at  $\times 10$  normal speed.
- [17] N. Darnton, L. Turner, K. Breuer, and H.C. Berg, Biophys. J. **86**, 1863 (2004).
- [18] B.V. Derjaguin, S.S. Dukhin, and A.A. Korotkova, Kolloid Zh. **23**, 53 (1961).
- [19] M.H. Robbins and R.S. Drago, Journal of Catalysis **170**, 295 (1997).